Synthesis of a novel carbon nanofiber structure for removal of lead

Hossein Faghihian*,†, Masoume Kooravand**, and Homa Atarodi*

*Department of Chemistry, Shahreza Branch, Islamic Azad University, Shahreza, Iran
**Young Researchers Club, Shahreza Branch, Islamic Azad University, Shahreza, Iran

Abstract−A new structure of carbon nanofibers was synthesized by chemical vapor deposition method. Kaolin was used as substrate and cyclohexanol and ferrocene as carbon source and catalyst, respectively. The morphology of the product was studied by scanning electron microscopy. Carbon nanofiber was modified with a mixture of nitric acid and sulfuric acid to enhance its adsorption capacity. The presence of functional groups on the treated adsorbent was assessed by FT-IR spectroscopy. The surface activity of the oxidized sample was estimated by Boehm's titration. The $pH_{(PZC)}$ of the samples was also measured. The adsorbent was then used for adsorption of Pb^{2+} at different experimental conditions. The optimized capacity of 211 $mg \cdot g^{-1}$ was obtained. Kinetic and thermodynamic of the reaction were studied. It was concluded that the adsorption process is spontaneous and endothermic. Equilibrium data were well fitted to the Langmuir model and the pseudo-second-order kinetic model described the adsorption process.

Key words: Carbon Nanofiber, Chemical Vapor Deposition, Lead, Adsorption, $pH_{(PZC)}$

INTRODUCTION

Carbon nanostructures show considerable adsorption capability, which is significantly influenced by the pH of the solution and the nanostructure surface properties. This property can be controlled by the treatment processing of the nanostructure [1]. Acidic oxidation methods have been widely reported as effective for purifying and functionalizing the surface of carbon nanostructures [2]. Oxygen containing functional groups (OH, C=O and COOH) can be introduced on carbon nanostructures through liquid-phase oxidation procedures. These functional groups attached on the surfaces of the carbon nanostructures promote carbon nanostructure chemical reactivity and improve their adsorption capability. The presence of heavy metals such as cadmium, copper, lead, nickel, mercury and zinc in aqueous environment may result in a major concern due to their toxicity and carcinogenicity, which may damage various systems of the human body [3]. Carbon nanostructures have been frequently studied as adsorbent for the removal of different heavy metal ions from liquid phases. Hu et al. [4] reported high adsorption capacities toward Pb(II) for a composite consisting of multi-walled carbon nanotubes/iron oxides/cyclodextrin. Modification of adsorbents including multiwalled carbon nanotubes by surfactants for removal of lead has also been reported [5,6]. Xu et al. [7] reported that the sorption of Pb(II) on oxidized multiwalled carbon nanotubes is strongly dependent on pH. Shao et al. [8] reported that chitosan grafted on multiwalled carbon nanotubes showed high adsorption capacity towards Pb(II). Wang et al. [9] reported that the adsorption property of multiwalled carbon nanotubes was improved by acidic treatment. They obtained maximum adsorption capacity of 85 mg/g for Pb(II), which was 20-fold greater than that obtained for untreated multi-walled carbon nanotubes. Leyva-Ramos et al.

[10] found that the adsorption capacity of activated carbon fibers depended on the surface properties of the adsorbent and was proportional to the concentration of carboxylic acid sites. Andrade-Espinosa et al. [11] reported that the modified nanofiber materials have a potential application in the removal of contaminants and recovery of precious metals present in aqueous phase. In this work, a new structure of carbon nanofibers was synthesized by chemical vapor deposition method on macroporous kaolin substrate surface using cyclohexanol and ferrocene as carbon source and catalyst, respectively. The process of synthesis involved the evaporation of a mixture of carbon precursor and ferrocene (mass ratio 20 : 1), in nitrogen atmosphere. The synthesized carbon nanofibers were modified by a mixture of nitric acid and sulfuric acid to enhance their cation adsorption capacity. The effect of experimental parameters such aspH, initial cation concentration, contact time and temperature on the adsorption of lead was also investigated.

MATERIALS AND METHODS

1. Synthesis and Oxidation of the Carbon Nanofibers

Macroporous kaolin disks were used as substrates. The disks were prepared by pressing a paste of kaolin and distilled water (mass ratio 70 : 30) and drying at 120 °C for 24 h followed by calcination at 800 °C for 3 h. The substrates were polished with 1,000 mesh sanding papers and then cleaned in an ultrasonic acetone bath for 30 min [12]. The kaolin substrate was placed in the middle of a horizontal furnace reactor (Fig. 1). At first, the reactor was purged with nitrogen to eliminate oxygen from the reaction chamber. The reactor was preheated to preset temperature; subsequently, the flask containing the mixture of carbon source and catalyst was heated and the vapors were purged by the nitrogen flow towards the high temperature zone of the reactor where the kaolin substrates were situated. Pyrolysis of the vapor took place and a film of carbon nanofibers was deposited on the substrate surface. After 30 min, the furnace
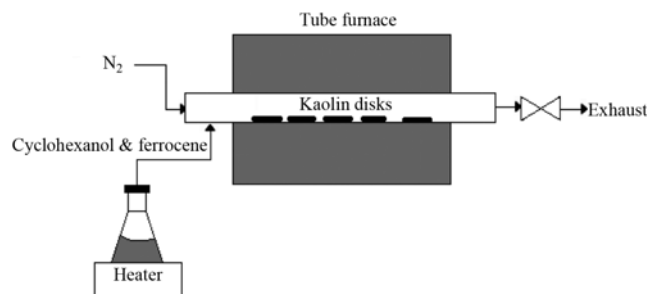
Fig. 1. Schematic diagram of the experimental CVD set-up.

was switched off and the reactor was cooled under nitrogen flow [13]. For the oxidative treatment, 0.1 g of the carbon nanofibers was mixed with 25 ml of acid mixture by mechanically stirring in a hot plate for 15 min at 60 °C. The mixture was then sonicated in an ultrasonic bath for 1 h. To minimize structural damage, a low power sonication bath and a relatively low acid exposure time were used [2]. These oxidized carbon nanofibers were used as adsorbent for removal of Pb^{+2} from aqueous solutions.

2. Boehm's Titration

Chemical oxidation of carbon nanofibers with mixture of nitric acid and sulfuric acid introduced different acidic functional groups on the surfaces and thus improved their hydrophilic and ion-exchange properties. To quantitatively estimate the functional groups on the surfaces of the oxidized carbon nanofibers, Boehm's titration method was used. This method is based on the fact that sodium hydrogen carbonate only neutralizes carboxyl groups, sodium carbonate neutralizes carboxyl groups and lactones, sodium hydroxide can neutralize carboxyl groups, lactones and phenols. So the different kinds of functional groups can be estimated through the known volume of used acid and bases. 0.02 g of the adsorbent was placed in asks containing 25 ml of 0.1 M sodium hydrogen carbonate, sodium carbonate and sodium hydroxide solutions. The asks were sealed and slowly shaken for 24 h. The solutions were then ltered and 10 ml of each ltrate was pipetted. The excess of bases was titrated with 0.1 M HCl. The acidic site concentration was determined from the amount of base solutions reacted with the appropriate function group on the carbon nanofiber surface [14]. The surface acidity of the as-synthesized and oxidized carbon nanofibers was quantied and presented in Table 1.

3. Point of Zero Charge Determination

The surface charge of the adsorbent depends on the pH of the surrounding electrolyte. There is a pH value, called 'point of zero charge' (PZC), at which the net surface charge is zero. The $pH_{(PZC)}$ of the as-synthesized and oxidized carbon nanofibers was determined as follows: 50 ml of 0.01 M NaCl solution was placed in a titration vessel at 298 K and nitrogen was bubbled through the solution to prevent the dissolution of CO_2. The pH was adjusted to a value between 3 and 9 by addition of 0.1 M HCl or 0.1 M NaOH
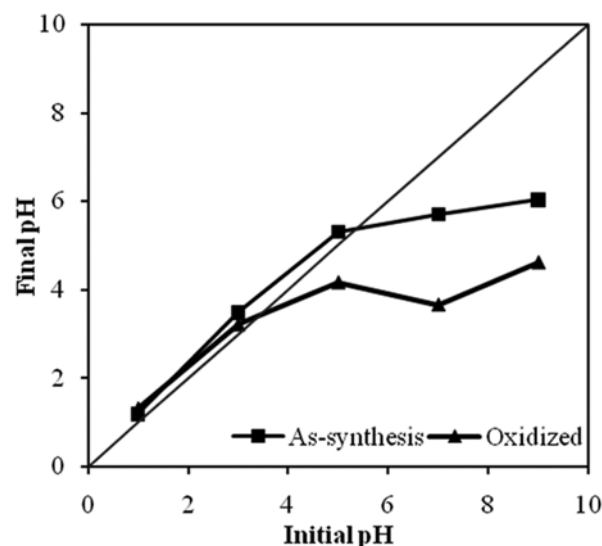

Fig. 2. The $pH_{(PZC)}$ of the carbon samples using the pH drift method.

solutions. 0.03 g of as-synthesized and oxidized carbon nanofiber was added to the solution and after 3 h, the final pH was measured and plotted against the initial pH [15]. The pH at which the bisector of the curve was crossed is the $pH_{(PZC)}$ of the adsorbent (Table 1 and Fig. 2).

4. Adsorbent Characterization

The morphology of carbon nanofibers was examined by a scanning electron microscope (AIS 2100, Japan). Fourier-transform infrared spectroscopy (FTIR) (Perkin Elmer Spectrum 65) in the frequency range of 4,000-400 cm^{-1} was used to study the changes on the surface after acidic treatment.

5. Batch Equilibrium and Kinetics Studies

Adsorption kinetics and equilibrium studies were conducted using batch technique by placing a known quantity of the adsorbent in polyethylene bottles containing 50 ml of Pb^{+2} solutions with predetermined concentration.

To evaluate the kinetic data, separate asks were prepared for each time interval and only one ask was taken for the desired time from 1 h to 24 h. For each adsorption isotherm, a known amount of the adsorbent was added to 50 ml of the solution in a concentration range of 100-500 mg/L. The effect of pH was also studied in the range of pH=1-6. Adsorption behavior of the samples was investigated at different temperatures of 25-35-45 and 55 °C.

In each experiment after the desired time, the solution and sorbent were separated by filtering and centrifugation and the concentration of lead in the solution was determined using a flame atomic adsorption spectrometer (Perkin Elmer 300). The following equation was employed:

$$q_e=(C_0-C_e)V/w \tag{1}$$

Table 1. Surface acidity and $pH_{(PZC)}$ of the as-synthesized and the oxidized carbon nanofibers

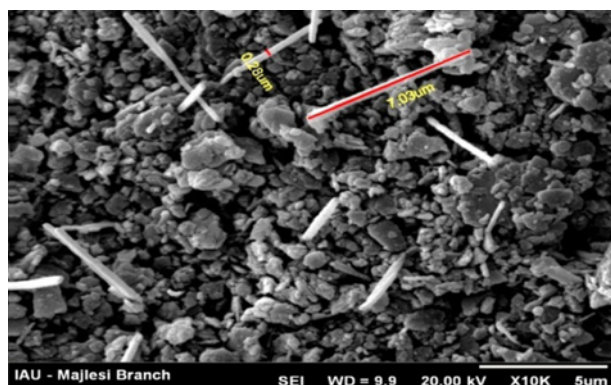| Material	Total acidic sites (mmol/g)	Carboxylic sites (mmol/g)	Phenolic sites (mmol/g)	Lactones sites (mmol/g)	$pH_{(PZC)}$
As-synthesis	2.21	0.42	1.08	0.71	5.6
Oxidized	6.63	0.63	3.8	2.2	3.37

Fig. 3. SEM image of carbon nanofiber.

Where q_e is the equilibrium adsorption uptake (mg/g), C_0 and C_e are the initial and equilibrium lead concentration (mg/L), respectively, V is the volume of the solution (L) and w is the mass of the adsorbent (g).

RESULTS AND DISCUSSION

1. Characterization of the Carbon Nanofibers

In different parts of the SEM images new structure of carbon nano fiber with mean diameter of 280 nanometer and lengths of a few hundreds were observed (Fig. 3). The synthesis of this structure has not been yet reported. The comparison of the infrared spectra of the initial kaolin disks (K_a), after synthesis of carbon nanofiber (K_b) confirmed that carbon nanofiber was synthesized. The FTIR of the K_c sample showed that hydroxyl and carboxylic acid groups are formed on the surface (Fig. 4). In K_a sample, the characteristic adsorption bands of Si-O and Si-O-Si elongation vibrations appeared around 1,082 cm^{-1}. The band at 815 cm^{-1} is attributed to the deformation vibrations of hydroxyl groups Al-O-H on the alumina surfaces. Lastly, the band at 480 cm^{-1} corresponds to Si-O-Al vibrations [16]. The above-mentioned bands remained in K_b and K_c samples, although some changes in the intensity were observed. In the K_b sample the adsorption band of OH stretching was observed around
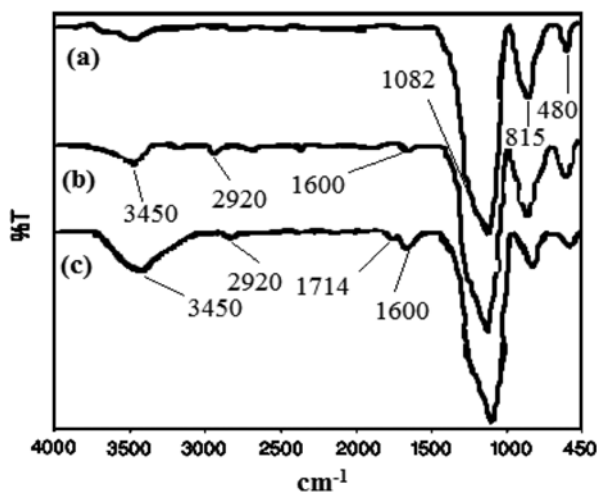

Fig. 4. FT-IR spectra of kaolin disk before nanofiber synthesis (a), after nanofiber synthesis (b) and after acidic treatment (c).

3,450 cm^{-1} and the CH$_2$ and conjugated C=C stretching bands appeared around 2,920 and 1,600 cm^{-1}, respectively. After the oxidative treatment (K_c), the same infrared spectrum was observed although some changes in the intensity were observed and in some cases, new peaks arose. A very small band that appeared at 1,714-1,726 cm^{-1} is assigned to stretching vibrations of carbonyl groups (C=O) of the carboxylic acids (RCOOH) [2].

The surface acidity of K_b and K_c was quantied by titration method and the results are presented in Table 1. It is important to mention that the oxidation of carbon nanofibers with oxidative agents preferentially introduces carboxylic groups into the structure although results show the phenolic and lactones groups were also produced (Table 1). This was in agreement with the finding reported by Donnet et al. for carbonaceous materials [17].

It is well known that the surface charge distribution of the materials depends on the dissociation of the surface functional group, which is strongly affected by the solution pH [12].

The pH$_{(PZC)}$ of the K_b and K_c samples is shown in Table 1 and Fig. 2. The pH$_{(PZC)}$ shifts to lower pH values after acidic treatment. These results indicated that there is equilibrium between negative and positive charges at pH 5.6 for K_b sample, whereas this was shifted to lower pH values (3.37) in acid modified samples. The amount and type of oxygen-containing surface groups and the pH of the solution determine the surface charge density, which directly determines the adsorption capacity of the material. For example, it has been reported that carboxylic acid groups dissociate in the pH interval of 3-6 [11]; this indicates that as the pH rises more carboxylic groups dissociate and hence the adsorption capacity of cations increases.

2. Sorption Mechanism

The mechanisms by which the metal ions are adsorbed onto carbon nanofibers are very complicated and appear attributable to electrostatic attraction, sorption precipitation and chemical interaction between the metal ions and the surface functional groups of carbon nanofibers. It is commonly believed that the chemical interaction between the metal ions and the surface functional groups of carbon nanofibers is the major sorption mechanism, so the performance is mainly determined by the nature and the concentration of these groups [18]. Pyrzynska [19] reported the protons of acidic groups of carbon nanofibers exchanged with the metal ions in aqueous phases. The solution pH dropped after sorption of metal ion onto carbon nanofibers reached equilibrium, which could be explained by the release of H$^+$ from the carbon nanofibers surface where metal ions are adsorbed, consequently decreasing the solution pH. The drop in pH value increased with a rise in initial metal ion concentration, which clearly indicates that sorption of more metal ion onto carbon nanofibers causes the release of more H$^+$ ions from the surface site of carbon nanofibers into the solution. This can be indicative of ion exchange process. Similar behavior was reported by Wang et al. [20] for adsorption of ^{243}Am(III) on the surface of multiwall carbon nanotubes. They also suggested that ion exchange mechanism was responsible for adsorption of ^{243}Am(III) on the adsorbent.

3. Effect of Contact Time

Fig. 5(a) shows the effect of contact time on the adsorption of Pb^{+2} onto oxidized carbon nanofibers. It was noted that the adsorption of Pb^{+2} was increased with time and then reached equilibrium. The contacting time to reach equilibrium was 8 h. The maximal capacity of 211 mg/g was obtained at C_0=250 mg/L.
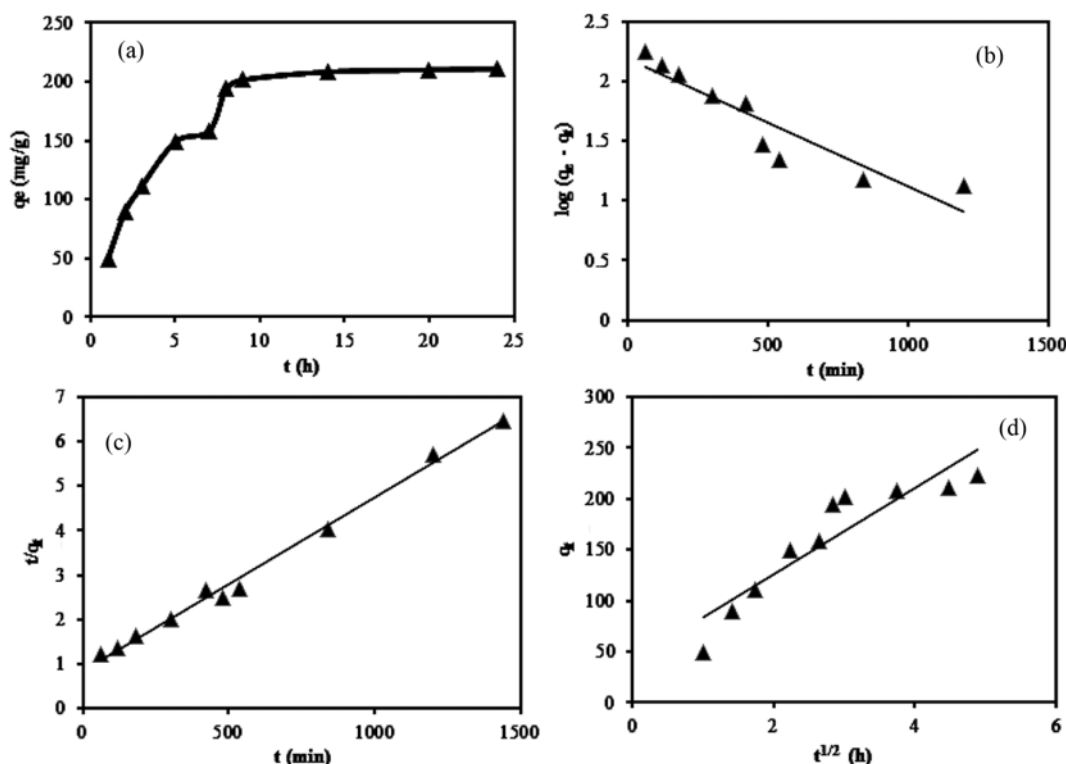
Fig. 5. Effect of contact time at 25 °C (V₀=50 ml, C₀=250 mg/L, pH=5.0, adsorbent=0.02 g) (a), Pseudo-first-order kinetic model at 25 °C (b), Pseudo-second-order kinetic model at 25 °C (c) and intra-particle diffusion model at 25 °C (d).

4. Kinetic Modeling

To analyze the adsorption kinetic parameters of lead onto the oxidized carbon nanofibers, three kinetic models including the pseudo-rst-order, the pseudo-second-order and the intra-particle diffusion models were applied.

The pseudo-rst-order kinetic model can be expressed in linear form [21]:

$$\log (q_e - q_t) = \log q_e - (k_1/2.303)t \tag{2}$$

where k_1 is the adsorption rate constant of rst order kinetic model, in min^{-1}, q_e and q_t, in mg/g, are equilibrium adsorption uptake (at time t=∞) and adsorption uptake (at time t), respectively.

The slope and the intercept of linear plot (Fig. 5(b)) are used to calculate the adsorption rate constants (k_1) and the amount of adsorption in equilibrium (q_e) and their results summarized in Table 2.

The pseudo-second-order kinetic model [22] can be expressed in linear form:

$$t/q_t = 1/k_2 q_e^2 + (1/q_e)t \tag{3}$$

where k_2 is the adsorption rate constant of second order kinetic model, in and $mg^{-1} \cdot min^{-1}$, q_e and q_t, in mg/g, are equilibrium adsorption uptake (at time t=∞) and adsorption uptake (at time t), respectively.

The slope and the intercept of linear plot in Fig. 5 care used to calculate the adsorption rate constants (k_2) and the amount of adsorption in equilibrium (q_e) and their results summarized in Table 2.

The intra-particle diffusion model is expressed by the following equation:

$$q_t = k_p t^{1/2} + C \tag{4}$$

where k_p is the intra-particle diffusion rate constant, in mg/g $h^{1/2}$, and C, in mg/g, is a constant related to the thickness of the boundary layer [22]. The intra-particle diffusion model parameters for adsorption of Pb^{+2} onto the oxidized carbon nanofibers were calculated, plotted in Fig. 5(d) and listed in Table 2. According to this model, if the plot of q_t versus $t^{1/2}$ gives a straight line, then intra-particle diffusion is involved in the adsorption process; and if this line passes through the origin then intra-particle diffusion is the rate-controlling step [23]. Ahmadzadeh Tofighi et al. [21] reported that the kinetics of adsorption varies with initial concentration of heavy metal ions. At lower initial concentration of heavy metal ions, adsorption is controlled by chemical adsorption, external diffusion and to some extent intra-particle diffusion (low R^2 values), while at higher initial concentration, desorption mainly involves intra-particle diffusion. At higher initial concentration, the mass transfer driving force is

Table 2. Kinetics parameters for adsorption of Pb^{+2} onto oxidized carbon nanofibers at 25 °C

Pseudo-second-order			Pseudo-rst-order			Intra-particle diffusion		
q_e	$K_2 \times 10^5$	R^2	q_e	$K_1 \times 10^3$	R^2	K_p	C	R^2
256.41	1.78	0.99	151.25	2.53	0.86	42.53	40.43	0.85

larger, and hence this results in higher diffusion rates of heavy metal ions within the pores of carbon nanostructures.

From Table 2, higher correlation coefficients indicated that the

Fig. 6. Effect of initial concentration on adsorption (V_0=50 ml, Time =8 h, pH=5.0, Adsorbent=0.02 g) (a), Freundlich isotherm model at 25 °C (b) and Langmuir isotherm model at 25 °C (c).

pseudo-second-order kinetic model fit the adsorption data better than the pseudo-first-order and intra-particle kinetic models.

5. Effect of Initial Cation Concentration

Fig. 6(a) shows the equilibrium adsorption uptake of Pb^{+2} by oxidized carbon nanofibers at different initial Pb^{+2} concentrations. As can be observed, increasing initial concentration signicantly increases the equilibrium adsorption uptake. It can be due to the fact that adsorption onto the oxidized carbon nanofibers is partially a diffusion-based process. At higher initial concentration, the mass transfer driving force is larger, and hence, this results in more adsorption of Pb^{+2} [21].

The adsorption capacity of Pb^{+2} attained 229 mg/g at initial concentration of 500 mg/L.

6. Adsorption Isotherms

Adsorption isotherm models are used to describe experimental adsorption data. The model parameters and the underlying thermo-dynamic assumptions of these adsorption models can provide some insight into the sorption mechanism, the surface properties and affinity of the adsorbent. Therefore, obtaining the 'best-fit' isotherm is very important. Freundlich and Langmuir isotherms were examined.

The Freundlich isotherm model can be expressed in a linear form:

$$\log q_e = n \log C_e + \log K_F \qquad (5)$$

where q_e is the equilibrium adsorption uptake of heavy metal ion, in mg/g, C_e is the equilibrium concentration of heavy metal ion, in mg/L, and K_F and n are the Freundlich parameters related to adsorption capacity and adsorption intensity, respectively. For n=1, the partition between the two phases is independent of the concentration. The situation n <1 is the most common and corresponds to a normal Langmuir isotherm, while n>1 is indicative of a cooperative sorption, which involves strong interactions between the molecules of adsorbates [24].

The slope and the intercept of the linear plot in Fig. 6(b) are used to calculate Freundlich parameters. The calculated adsorption isotherms parameters are listed in Table 3. Deviation of the n value from unity indicates a non-linear adsorption that takes place on heterogeneous surface. The n values are smaller than 1, which indicates favorable adsorption of Pb^{+2} onto the oxidized carbon nanofibers.

The equation of the Langmuir adsorption model can be expressed in a linear form:

$$C_e/q_e = 1/q_m K_L + C_e(1/q_m) \qquad (6)$$

where q_e is the equilibrium adsorption uptake of heavy metal ion, in mg/g, C_e is the equilibrium concentration of heavy metal ion, in mg/L, q_m is the maximum adsorption capacity corresponding to the complete monolayer coverage, in mg/g, and K_L is the Langmuir constant which is related to the energy of adsorption.

An essential characteristic of Langmuir isotherm can be expressed by a dimensionless constant called equilibrium parameter:
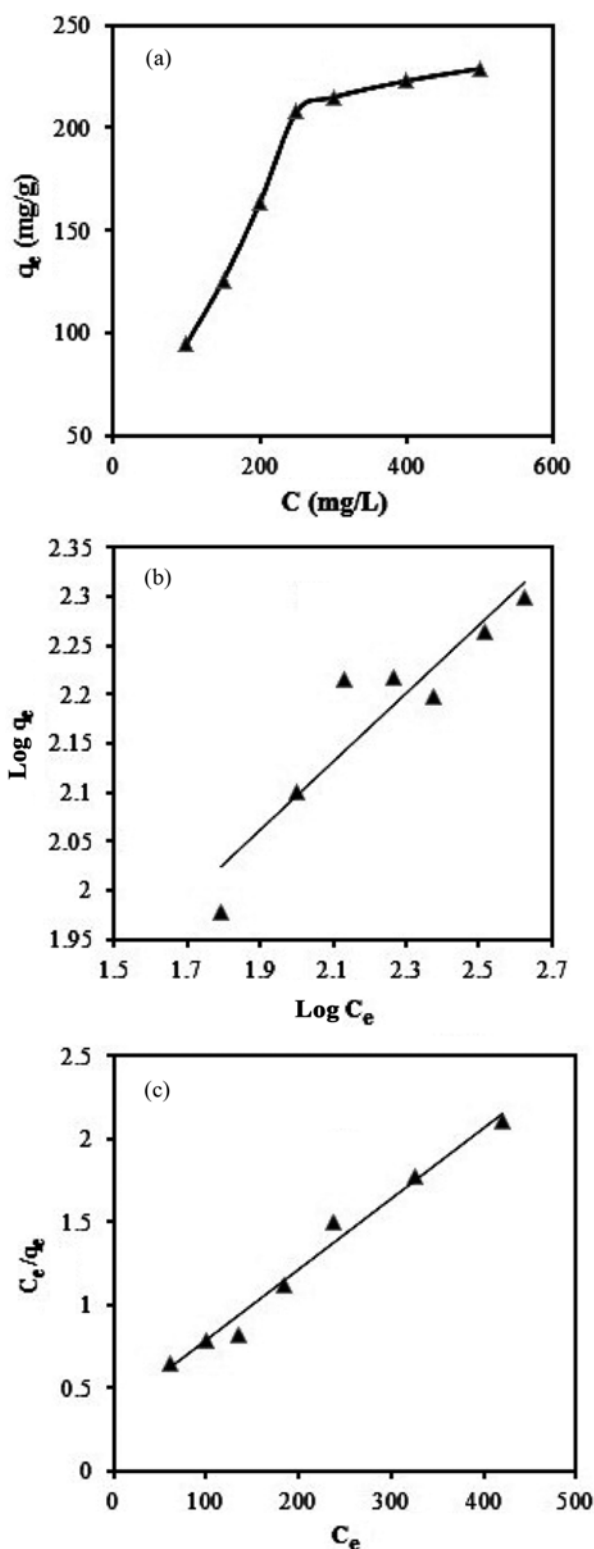
Table 3. Adsorption isotherm parameters for adsorption of Pb^{+2} onto oxidized carbon nanofibers at 25 °C

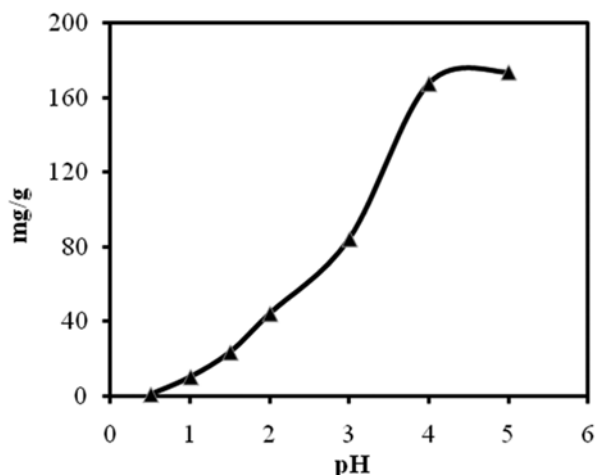| Langmuir			Freundlich		
q_m	K_L	R^2	n	K_F	R^2
232.56	0.01	0.98	0.3	25.23	0.87

Fig. 7. Effect of contacting pH on adsorption of Pb^{+2} with oxidized carbon nanofibers (V$_0$=50 ml, C$_0$=250 mg/L, contacting time =8 h, Adsorbent dosage=0.02 g).

$$R_L=1/(1+K_LC_0) \tag{7}$$

Where K$_L$ is the Langmuir constant and C$_0$ is the highest initial heavy metal ions concentration, in mg/L. The value of R$_L$ indicates the type of the isotherm to be either unfavorable (R$_L$>1), linear (R$_L$=1), favorable (0<R$_L$<1) or irreversible (R$_L$=0) [21].

The slope of the linearized Langmuir plot was used to calculate the adsorption constants (Fig. 6(c) and Table 3). From Table 3, higher correlation coefficients indicated that the Langmuir model fit the adsorption data better than the Freundlich model.

7. Effect of pH

The removal of Pb^{+2} from aqueous solution by oxidized carbon nanofibers was found to be highly dependent on the solution pH value, which aects the surface charge of the adsorbent and degree of ionization and speciation of the adsorbates. Fig. 7 shows that the Pb^{+2} adsorption capacity of the oxidized carbon nanofibers increases with the pH value from 0.5 to 5.0. Precipitation will occur as the pH exceeds to 5.5. At pH values higher than the pH$_{(PZC)}$, a larger amount of oxygen-containing surface groups are dissociated, thus generating a more negative surface favorable to sequester, by electrostatic interactions, positively charged species present in solution. The opposite is expected to happen at pH values lower than the pH$_{(PZC)}$ [11]. At pH>pH$_{(PZC)}$, the positively-charged metal ions can be adsorbed on the negatively-charged oxidized carbon nanofibers, so sorption of metal ions generally increases with increasing pH. The low adsorption that occurs in acidic solutions can be attributed in part to the competition between hydrogen and metal ions on the same carbon nanofiber sites. In some cases, when a higher pH is employed, both sorption and precipitation are involved in the removal of metal ions from aqueous solution. It was suggested that the use of appropriate dimensions of carbon nanofibers may support the trapping process of the precipitated metal hydroxides [19].

8. Effect of Temperature

It is well known that temperature is an important parameter in the adsorption process of metal ions. Increasing temperature results in a rise in diffusion rate of metal ions across the external boundary layer and within the pores of carbon nanofibers due to the result of
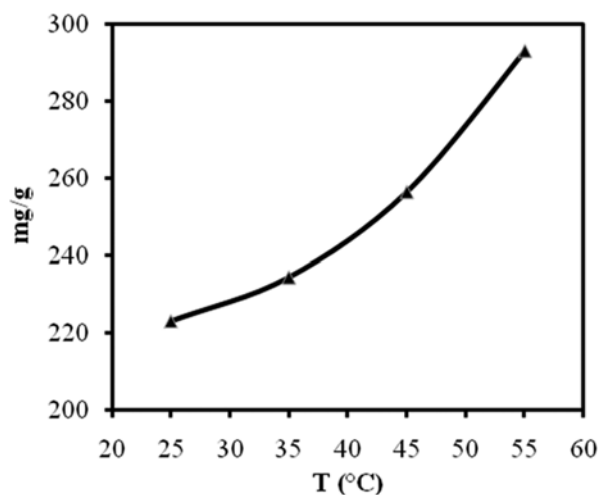

Fig. 8. Effect of solution temperature on adsorption of Pb^{+z} with oxidized carbon nanofibers.

decreasing solution viscosity [18]. The effect of temperature on the removal of Pb^{+2} to oxidized carbon nanofibers was investigated at four different temperatures: 25, 35, 45 and 55 ℃ (Fig. 8). The results show that the adsorption of Pb^{+2} increases with increasing temperature.

9. Thermodynamic Parameters

The change in Gibbs free energy, enthalpy and entropy of adsorption were calculated by using the following equations:

$$K_d=q_e/C_e \tag{8}$$

$$\Delta G^0=\Delta H^0-T\Delta S^0 \tag{9}$$

According to Van't Ho equation:

$$\ln K_d=\Delta S^0/R-\Delta H^0/RT \tag{10}$$

where R is gas constant (8.314 J/molK) and K$_d$ is the equilibrium constant and T is the temperature in K [21].

The plot of lnK$_d$ versus 1/T was linear. Negative values of ΔH^0 showed the endothermic nature of adsorption (Fig. 9). The negative values of ΔG^0 indicated that the adsorption process led to a decrease in Gibbs free energy and that the adsorption process was feasible
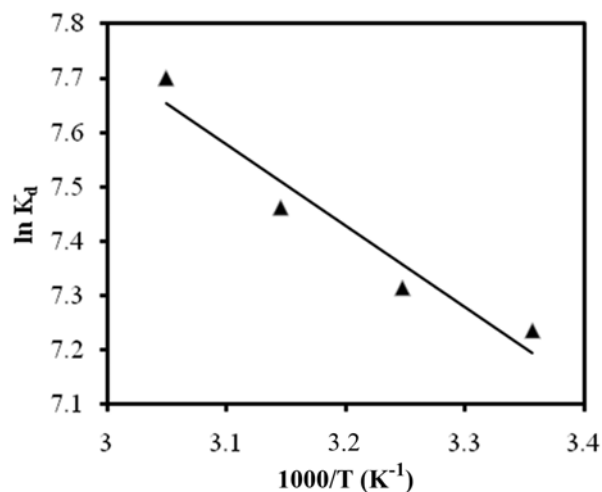

Fig. 9. Plot of lnK$_d$ versus (1/T) according to Eq. (10).

Table 4. Thermodynamic parameters for adsorption of Pb^{+2} onto oxidized carbon nanofibers

R^2	ΔG°				ΔS°	ΔH°
	55 °C	45 °C	35 °C	25 °C		
0.94	−33322.2	−32305.9	−31289.6	−30273.3	101.63	12.46

and spontaneous for Pb^{+2} at 25, 35, 45 and 55 °C. The positive values of ΔS^0 suggested the increased randomness at the solid/solution interface during the adsorption of Pb^{+2} on adsorbents. This result is consistent with the results obtained in [25]. The thermodynamic parameters for the removal of Pb^{+2} are given in Table 4.

CONCLUSION

Chemical vapor deposition was used for synthesis of carbon nanofibers. The carbon nanofibers were then oxidized with mixture of nitric acid and sulfuric acid at room temperature. The nature of the surface was changed after acidic treatment, including an increase in surface functional groups oxygen containing positive and negative charges, which made carbon nanofibers adsorb more positive ions. Hence, the adsorption capacity of the carbon nanofibers increased signicantly after the oxidation process. Boehm's titration was a suitable method for estimation of surface activity. Adsorption capacity was also affected by several parameters, including initial concentration, pH, and contact time. Thermodynamic studies showed that the adsorption process was endothermic and spontaneous. The synthesis of new structure and the higher adsorption capacity are the most advantageous results of this research.

REFERENCES

1. P. Liang, Q. Ding and F. Song, *Sep. Sci.*, **28**, 2339 (2005).
2. F. Aviles, J. V. Cauich-Rodriguez, L. Moo-Tah, A. May-Pat and R. Vargas-Coronado, *Carbon*, **47**, 2970 (2009).
3. Y. H. Li, S. Wang, J. Wei, X. Zhang, C. Xu, Z. Luan, D. Wu and B. Wei, *Chem. Phys. Lett.*, **357**, 263 (2002).
4. J. Hu, D. Shao, C. Chen, G. Sheng, J. Li, X. Wang and M. Nagatsu, *J. Phys. Chem. B*, **114**, 6779 (2010).
5. J. Li, S. Chen, G. Sheng, J. Hu, X. Tan and X. Wang, *Chem. Eng. J.*, **166**, 551 (2011).
6. D. Shao, Z. Jiang and X. Wang, *Plasma Process Polym.*, **7**, 552 (2010).
7. D. Xu, X. Tan, C. Chen and X. Wang, *J. Hazard. Mater.*, **154**, 407 (2008).
8. D. Shao, J. Hu and X. Wang, *Plasma Process Polym.*, **7**, 977 (2010).
9. H. J. Wang, A. L. Zhou, F. Peng, H. Yu and L. F. Chen, *Mater. Sci. Eng. A*, **466**, 201 (2007).
10. R. Leyva-Ramos, M. S. Berber-Mendoza, J. Salazar-Rabago, R. M. Guerrero-Coronado and J. Mendoza-Barron, *Adsorption*, **17**, 515 (2011).
11. G. Andrade-Espinosa, E. Munoz-Sandoval, M. Terrones, M. Endo, H. Terrones and J. R. Rangel-Mendez, *J. Chem. Technol. Biot.*, **84**, 519 (2009).
12. T. Mohammadi, M. Ahmadzadeh Tofighi and A. Pak, *Int. J. Chem. React. Eng.*,**7**, A75, 1 (2009).
13. S. Musso, G. Fanchini and A. Tagliaferro, *J. Diam. Relat. Mater.*, **14**, 784 (2005).
14. M. Kandah and J. Meunier, *J. Hazard. Mater.*, **146**, 283 (2007).
15. J. Rivera-Utrilla, I. Bautista-Toledo, M. A. Ferro-Garcia and C. Moreno-Castilla, *J. Chem. Technol. Biot.*,**76**, 1209 (2001).
16. X. Xia, X. Zeng, J. Liu and W. Xu, *J. Appl. Polym. Sci.*, **118**, 2461 (2010).
17. J. B. Donnet, *Carbon*, **6**, 161 (1968).
18. G. P. Rao, C. Lu and F. Su, *Sep. Purif. Technol.*, **58**, 224 (2007).
19. K. Pyrzynska, *TrAC Trend. Anal. Chem.*, **29**, 718 (2010).
20. X. Wang, C. Chen, W. Ding, D. Xu and X. Zhou, *Environ. Sci. Technol.*, **39**, 2856 (2005).
21. M. Ahmadzadeh Tofighy and T. Mohammadi, *J. Hazard. Mater.*, **185**, 140 (2011).
22. C. Chen and X. Wang, *Ind. Eng. Chem. Res.*, **45**, 9144 (2006).
23. J. P. Chen, S. Wu and K. H. Chong, *Carbon*, **41**, 1979 (2003).
24. J. Hu1, S. W. Wang, D. D. Shao, Y. H. Dong, J. X. Li and X. K. Wang, *The Open Environmental Pollution & Toxicology J.*, **1**, 66 (2009).
25. Y. H. Li, Z. Di, J. Ding, D. Wu, Z. Luan and Y. Zhu, *Water Res.*, **39**, 605 (2005).